IOPscience iopscience.iop.org

Home Search Collections Journals About Contact us My IOPscience

Density functional theory and beyond—opportunities for quantum methods in materials modeling semiconductor technology

This article has been downloaded from IOPscience. Please scroll down to see the full text article.

2008 J. Phys.: Condens. Matter 20 064232

(http://iopscience.iop.org/0953-8984/20/6/064232)

View the table of contents for this issue, or go to the journal homepage for more

Download details:
IP Address: 129.252.86.83
The article was downloaded on 29/05/2010 at 10:32

Please note that terms and conditions apply.

J. Phys.: Condens. Matter **20** (2008) 064232 (9pp) doi:10.1088/0953-8984/20/6/064232

Density functional theory and beyond—opportunities for quantum methods in materials modeling semiconductor technology

Sadasivan Shankar, Harsono Simka and Michael Haverty

Process Technology Modeling, Design and Technology Solutions, Technology and Manufacturing Group, Intel Corporation, 2200 Mission College Boulevard, Santa Clara, California-95052, USA

Received 23 November 2007, in final form 12 December 2007
Published 24 January 2008
Online at stacks.iop.org/JPhysCM/20/064232

Abstract
In the semiconductor industry, the use of new materials has been increasing with the advent of nanotechnology. As critical dimensions decrease, and the number of materials increases, the interactions between heterogeneous materials themselves and processing increase in complexity. Traditionally, applications of *ab initio* techniques are confined to electronic structure and band gap calculations of bulk materials, which are then used in coarse-grained models such as mesoscopic and continuum models. Density functional theory is the most widely used *ab initio* technique that was successfully extended to several applications. This paper illustrates applications of density functional theory to semiconductor processes and proposes further opportunities for use of such techniques in process development.

(Some figures in this article are in colour only in the electronic version)

1. Introduction

Nanoscience is the understanding of science at the nanolevel, where quantum mechanics provides self-consistent explanation for most practical applications of relevance. In contrast, nanotechnology is defined (M Roco, 2000) as *research and technology development at the atomic, molecular or macromolecular levels, in the length scale of approximately 1–100 nm range*. R Feynman's talk in APS in 1959 initiated the advent of this revolution [1]. '*There is plenty of room at the bottom*: . . . .*In the year 2000, when they look back at this age, they will wonder why it was not until the year 1960 that anybody began seriously to move in this direction*. . .'. The key to note here is the overlap of molecular and structural scales lead to material behavior determined by the details at the structural level.

Given the globalization of the marketplace, technology leadership in the fundamental sciences and engineering areas needs renewed vigor similar to the advent and innovation of plastics industry and the semiconductor industry of the 20th century. Nanotechnology is expected to impact nearly every industry. The US National Science Foundation predicted the global market for nanotechnologies will reach $1 trillion in a couple of decades. The research community and various industries are pursuing hundreds of applications in nanomaterials, nanoelectronics, and biotechnology (e.g. [3]). Most near term (1–5 years) applications of nanotechnology are expected to be in nanomaterials. These include materials such as lighter and stronger nanocomposites, antibacterial nanoparticles, and nanostructured catalysts. Nanodevices and nanoelectronics are further off, perhaps 5–15 years, with applications in faster computers, sensors, and medical diagnostics.

The multi-billion dollar semiconductor industry behind the information technology (IT) revolution is driven by rapid progress in semiconductor process development and manufacturing technology. Process development in turn is guided by an empirical observation widely known as Moore's law (figure 1). The law observed that the number of transistors in a given area doubles every 18–24 months. This law has held for 42 years and resulted in the current generation of multi-core processors ushering in supercomputing power to the desktops. A recent consequence of Moore's law is features with dimensions of several tens of nanometers [4, 5]. As the

 © 2008 IOP Publishing Ltd Printed in the UK

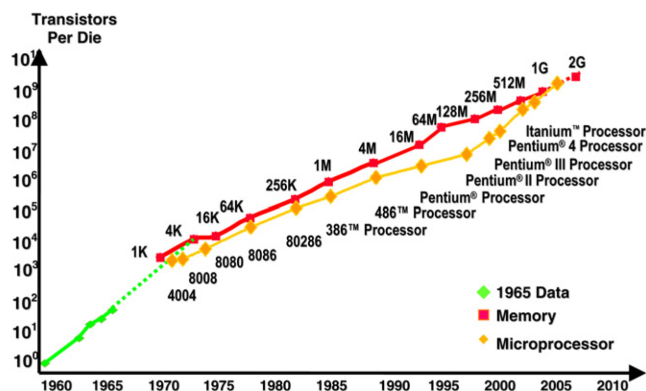

Figure 1. Moore's law (Source: Intel).

domain size itself reaches the same order of magnitude as the current technology node of 45 nm, material effects become dominant. We believe 45 nm is the tipping point of multiple materials applications in semiconductor industry.

The nanometer regime is characterized by the increasing influence of quantum effects on properties since the material domains coincide with the critical dimension. For example, the mean free path in metallic interconnects is ∼40 nm, grain size in polycrystalline materials is ∼20 nm, filler dimensions used in polymers are ∼20 nm, and void dimensions are ∼10 nm. Devices, structures (such as nanotubes which are being considered for switching devices and interconnects), domains (e.g. pores and grain boundaries), and thin films are tens of nanometers in size (figure 2). Overlap of these domains leads to convergence of molecular, condensed matter, and mesoscopic laws of physics leading to properties that do not manifest in bulk materials.

In the absence of modeling, empirical experimentation is used to characterize and drive technology development. This process is both expensive and time-consuming. More importantly, the specific operating window identified experimentally may not be globally optimal. Modeling aids in quantifying the relationships between causes and effects. This in turn enables systematic design of experiments for optimizing the process that could be used to accelerate the learning. A methodology of concurrent application of modeling and experiments played a critical role in Intel for at least the last two decades. A faster rate of learning provides compelling reasons for materials modeling even in semiconductor companies where the product is not new materials, but new devices. For the two applications we address in this paper, we focus on applying quantum methods to gas and solid phase modeling. Description of models in atomic and mesoscopic scales is beyond the scope of this discussion, and is briefly addressed in the conclusions.

The models which cover these domains are mostly based on quantum methods that solve the Schrödinger equation in $3N$ dimensions, where N is the number of electrons in the system. Given that most devices consist of condensed matter, N is on the order of 10^{23}. This makes solving the equations for practical application intractable. As a result, the most widely used technique is density functional theory (DFT) in which the $3N$-dimensional system reduces to three-dimensional problems [6, 7]. One of the most widely used approximations is the local density approximation (LDA) where functions of local electron densities approximate the exchange potentials leading to a three dimension formulation. More accurate approximations such as generalized gradient approximations (GGA) increase the applicability of DFT methods. The approximations are generally of two types, one in which the density functions are systematically improved to capture more and more non-local features of the wave functions (e.g. local density approximation, generalized gradient approximation) and the second one in which the exchange–correlation functionals are approximated by rigorous models (e.g. many body perturbation theory).

2. Applications

2.1. Atomic layer deposition

Atomic layer deposition (ALD) is an increasingly attractive option for deposition of various crucial semiconductor material layers, including high-k dielectrics and barrier layer in semiconductor interconnect applications. ALD is a gas phase deposition process typically consisting of two half-reactions, each involving a chemical or precursor. The precursor gases are introduced separately into the reactor for film growth with sequential pulses. ALD growth is self-limiting since the availability of gas phase reactants controls the process, leading to excellent thickness control and film conformality. Examples of the desired growth behavior are the precise thickness control and sharp interfaces in ZrO_2 high-k films grown on SiO_2 [11] (figure 3), and the conformality of Al_2O_3 ALD-grown film in patterned features [12] (figure 4). Experimental characterizations of ALD surface reactions are difficult and time-consuming, due to the process complexity as illustrated by the disparity in timescales (figure 5). As a result, modeling, particularly those based on first-principles simulations, is an attractive option to investigate the surface chemistry and in determining how precursor reactivity affects ALD performance [8].

We investigated ALD reaction pathways as described below. The system of interest was ALD of Al_2O_3 using trimethylaluminum (TMA) and H_2O precursors. The overall reaction was deposition of Al_2O_3 with CH_4 byproducts:

$$2(CH_3)_3Al + 3H_2O \rightarrow Al_2O_3 + 6CH_4$$

with 'binary' sequence of TMA and H_2O exposures:

$$Al(CH_3)_3(g) + OH^* \rightarrow AlO(CH_3)_x^* + CH_4(g)$$

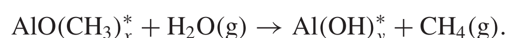

$$AlO(CH_3)_x^* + H_2O(g) \rightarrow Al(OH)_y^* + CH_4(g).$$

The deposition process involved removal of the TMA methyl ligands after reaction with H_2O, leaving methane on the surface. Our modeling goal was to determine the mechanism for the overall reaction, energetics, and reaction rates associated with each step. For surface reactions, we represented the Al_2O_3 surface using simple cluster structures, as shown in figure 6. We treated the various sites considered relevant in the

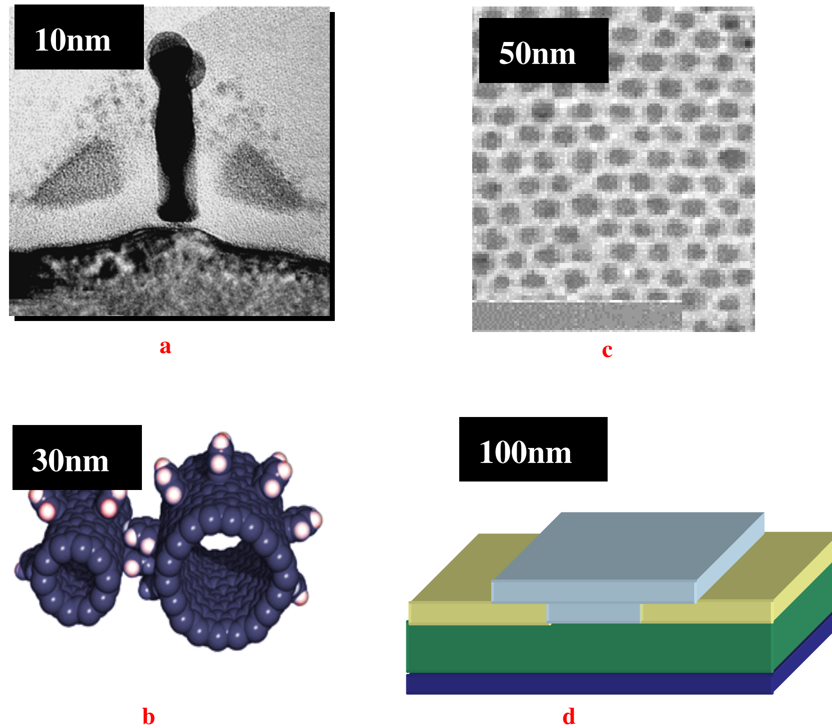

Figure 2. Overlap of length scales; (a) nanodevice–transistor, (b) nanostructure–carbon nanotube, (c) nanodomain–porous dielectric, (d) thin film.

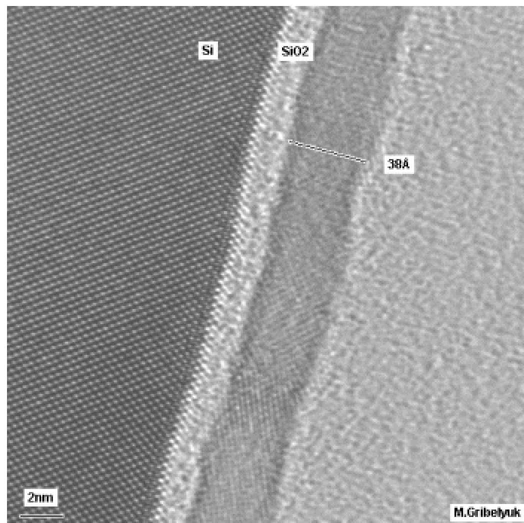

Figure 3. An example of accurate control of thickness during an ALD process: high resolution TEM of ZrO_2 ALD-deposited film on SiO_2 [10].

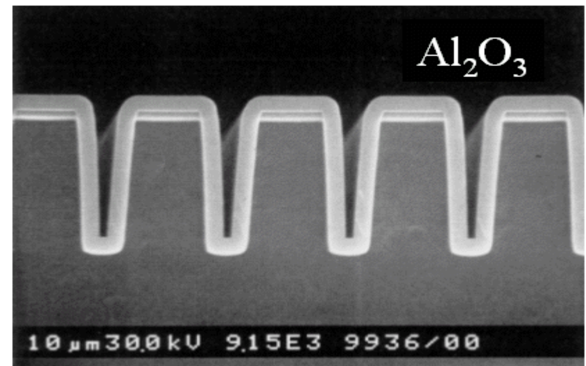

Figure 4. An example of excellent conformality and step coverage during an Al_2O_3 ALD process [11].

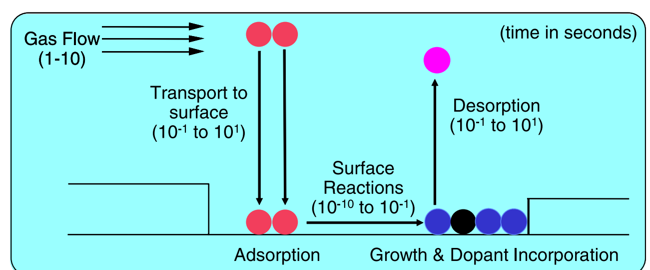

Figure 5. Summary of timescales involved in ALD process.

reactions of the precursors using different clusters. For the half-reaction of the TMA precursor, the three important surface sites were the Al–OH, the Al–$(CH_3)_2$, and the Al–(CH_3) sites. Hydrogen atoms terminated the bonds, in each of these clusters (figure 6). The small clusters included only one Al atom bonded to either one, two, or three hydroxyl groups, depending on the type of the site. To depict an 'empty' surface, the Al atom was bonded to three –OH groups, representing three active Al–OH sites. The large clusters included more than one Al atom and included the effect of Al–O surface bonds. For example, the Al–OH site was represented by an Al–OH

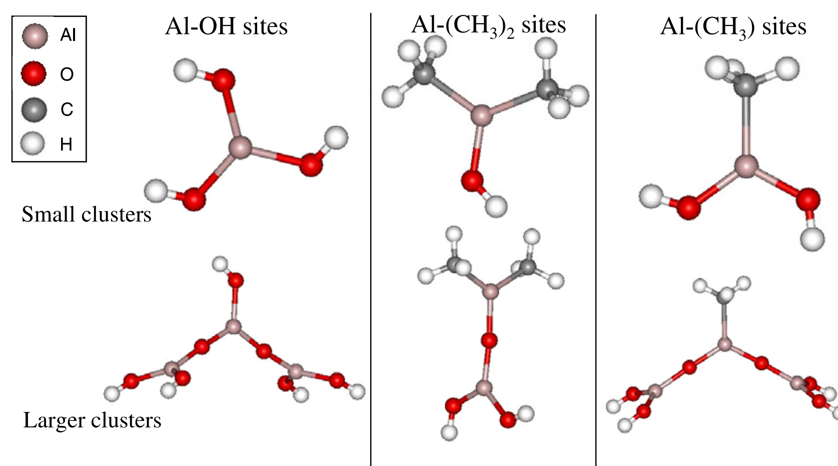

Figure 6. Cluster models used in DFT simulations of Al_2O_3 ALD process.

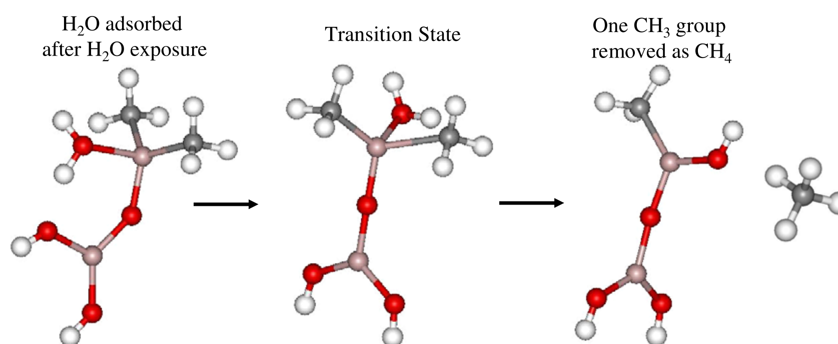

Figure 7. Investigation of Al_2O_3 ALD reaction pathways using DFT: removal of ligand from trimethylaluminum (TMA) precursor.

bond connected to two –(O–Al(OH)$_2$) groups (bottom left of figure 6). While these clusters did not represent all possible reactive sites or reactive bonds on the Al_2O_3 surface, they provided useful insight into the main reaction pathways involving TMA and H_2O. Additional clusters were created to probe more complex reaction paths on the Al_2O_3 surface.

The kinetics of surface reactions determines the operating conditions needed for a successful ALD process. Activation or decomposition of ALD precursors requires sufficient energy to occur, which is typically supplied to the reactor by thermal heating or plasma activation. The overall kinetic barrier for ALD precursor reactions dictates the operating temperature for a thermal ALD process. Too low a temperature leads to unacceptably slow deposition rates and high impurity levels in the film due to incomplete ligand removal. Too high a temperature may lead to precursor decomposition in the gas phase and a loss of self-limiting behavior, as well as poor film properties due to agglomeration or other surface processes. We used DFT simulations to investigate the kinetic barrier for ALD reaction steps. One example in Al_2O_3 ALD is summarized in figure 7, where DFT was used to locate the transition state in the reaction of surface CH_3 removal by H_2O after an H_2O exposure step. In this case, the adsorbed H_2O rearranged so that one H atom moved closer to the CH_3 group, and eventually left the surface as CH_4. The reaction barrier height (energy of transition state (middle) relative to the stable adsorbed configuration (left)) was 22 kcal mol^{-1}. We used the B3LYP hybrid DFT method and a triple-zeta basis set with polarization and diffuse functions (6-311 + G(d, p)) [12, 13].

We investigated the main ALD reaction pathways for deposition of Al_2O_3 and removal of undesired carbon impurities via desorption of CH_4 (summarized in figures 8 and 9). TMA precursors in the gas phase adsorbed on a –OH terminated Al_2O_3 surface; the Al atom in TMA formed a bond with the O atom in the surface –OH group, stabilizing the TMA by 4.5 kcal mol^{-1} (Gibbs free energy of reaction at 298 K). The adsorbed TMA precursor then underwent internal rearrangement, leading to CH_4 removal. We used DFT simulations with the B3LYP/6-311 + G(d, p) method [13] to identify the transition state for this reaction. The transition state structure (the third structure from the left on figure 8) was a four-membered center (Al–O–H–C), with an energy barrier of 11.7 kcal mol^{-1}. While the energy barrier was not very high, the Al_2O_3 ALD process must be thermally activated (the deposition temperature must be higher than 298 K). Another product of this surface reaction was dimethylaluminum species bonded to the surface and formation of an additional Al–O–Al bond. CH_4 removal was thermodynamically favorable ($\Delta G_{\text{rxn},298\text{ K}} = -38.4$ kcal mol^{-1}). The dimethylaluminum underwent further reactions with additional –OH groups or

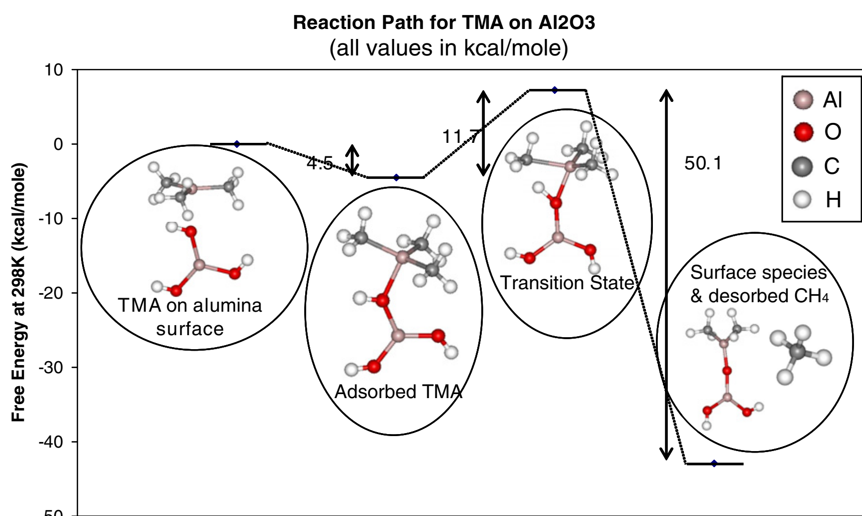

Figure 8. Reaction pathway of adsorbed trimethylaluminum in Al_2O_3 ALD.

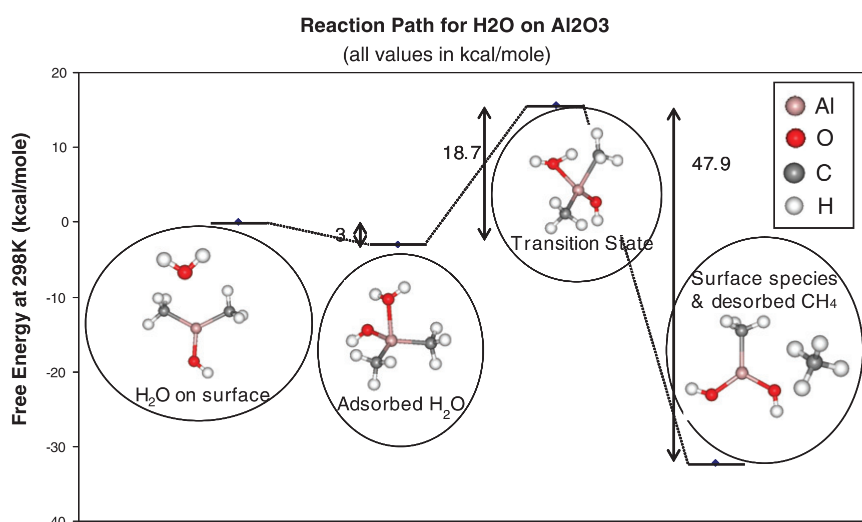

Figure 9. Reaction pathway of H_2O in Al_2O_3 ALD.

with the H_2O precursor molecules in the next ALD pulse step, and liberated additional CH_4 molecules.

We modeled the H_2O reaction sequence as a weak adsorption of H_2O molecule on Al_2O_3 surface saturated by adsorbed dimethylaluminum, followed by internal rearrangement of the surface complex to form a H–CH_3 bond that led to CH_4 removal. The energetics is summarized in figure 9. The transition state structure was identified, with an energy barrier of 18.7 kcal mol^{-1}, which was higher than the energy barrier for the TMA reaction. We investigated the removal of the remaining CH_3 group by H_2O using the same approach, and developed a detailed surface reaction mechanism for Al_2O_3 ALD. This mechanism was used in continuum based ALD reactor simulations, which included effects of fluid flow, mass and heat transport, and chemical kinetics. As an example, simulations predicted Al_2O_3 'staircase' growth behavior (figure 10) in a well-characterized viscous flow reactor [9]. The figure on the left shows the quartz microbalance measurements of Al_2O_3 growth, while the figures on the middle and the right side show the simulation results, in which a reactor model with rigorous descriptions of the gas flow, diffusion, and reactions used the reaction rates from the DFT calculations. The model predicted an Al_2O_3 growth rate of 1.2 Å/cycle for deposition at 177 °C, 1 Torr pressure, in good agreement with the measured value of 1.07 Å/cycle as seen in figure 10. The predicted growth curve also suggested there was no incubation period for Al_2O_3 growth on –OH terminated alumina substrate, consistent with observations. Having an accurate ALD reaction mechanism enabled an effective model based optimization of the effects of process conditions (temperature, pressure, precursor dose, and flow rates) and reactor design on ALD performance. The analysis from these results may be used in two ways: to optimize the process by specific precursor design and reactor re-design. Both may provide directions to technology development teams for more efficient process options by improving thickness uniformity and increasing throughput.

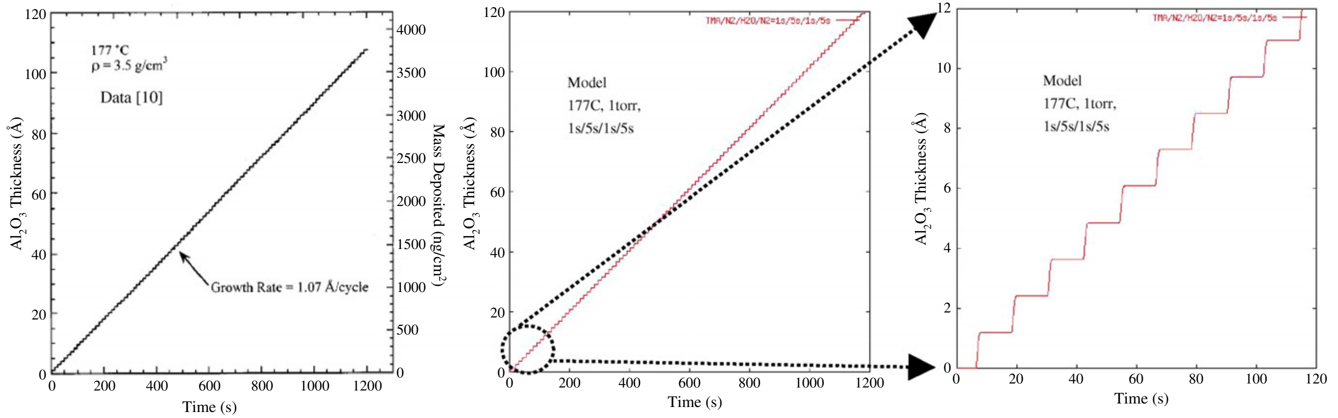

Figure 10. Modeling results for Al_2O_3 ALD growth in a viscous flow reactor, model predicted 'staircase' like growth, consistent with experimental data [9].

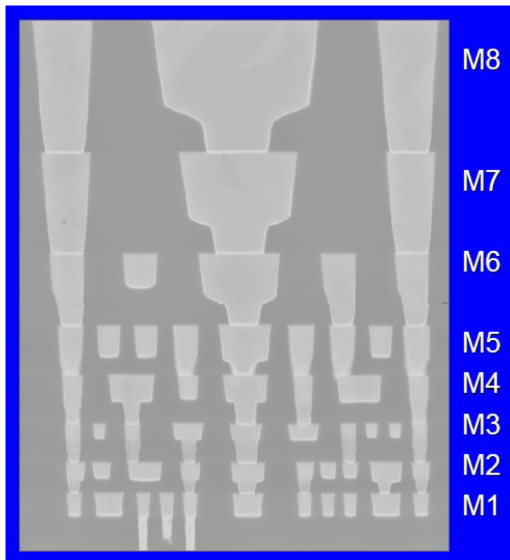

Figure 11. SEM cross section showing the eight metallization layers of Intel 65 nm technology.

2.2. Interface adhesion

Intel's 65 nm logic technology features eight Cu interconnect layers with carbon-doped oxide (CDO) low-K inter-layer dielectric (ILD) and silicon carbide/nitride etch stop layers, as illustrated in figure 11 [14]. Such advanced back-end interconnect technologies contain dual-damascene Cu layers and numerous interfaces with a wide variety of materials. Understanding the interface is critical to optimization and ensuring that the devices have the desired properties and reliability. In this work we focused on the interaction of Cu metallization interfaces with the etch stop and barrier layers.

Many challenges exist in characterizing multi-material interface properties such as adhesion. The adhesion strength depends on factors such as chemical bonding between interface materials or the processing conditions. Due to the buried nature of these interfaces and their small scale, any characterization often suffers from a lack of details of composition, interface morphology, or structure. Adhesion measurements themselves require complex metrology, which must correctly take into account the failure mechanism mode/type and sample geometry, resulting in slow turn-around. In practice, the adhesion of a multi-layered structure is limited by the weakest material or interface, hence making it difficult to probe the impact of design changes on the stronger interfaces.

The complex interactions of all factors make it difficult to deconvolve and evaluate each aspect separately. For these reasons, our goal was to develop a fundamental model for screening Cu interface adhesion to guide experiments. Our earlier work with this model captured the observed behavior of adhesion between Cu with SiC and Cu with Si_3N_4 validated by experimental trends [2]. We used the following equation to evaluate adhesion from DFT:

$$E_{\text{adhesion}} = (E_{\text{stack}} - E_{\text{slab1}} - E_{\text{slab2}})/A$$

E_{stack} was the total energy of the relaxed stack, E_{slab1} was the total energy of slab1, E_{slab2} was the total energy of slab2, and A was the cross sectional interface area.

In addition to the traditional 4-pt bend adhesion characterization metrology, the interface energy may also be related to the wetting of materials on Cu. In the case of Cu deposition on the barrier, we were interested in the relative wetting of Cu on Ta. In our previous paper we demonstrated that the surface affinity of Cu on a variety of barrier interfaces correlated with wetting of various barrier metal options [2]. In addition, we showed that beta-Ta(001) was superior to TaN, TaC, TaO, TiNSi, TiNC, W(111), and TiN(111). This was subsequently validated experimentally in the superior wetting character of Ta versus TaN, TiN and TiNSi as shown in figure 12.

We extended our adhesion analysis further to be more quantitative to calculate the adsorption energy of Cu on Ta with beta-Ta as the structural model. We estimated the adsorption energy by placing a single Cu atom on the Ta surface at varying distances to the surface and calculated the adsorption energy of the system. This adsorption energy was the difference of the supercell energy of the Cu atom near the Ta surface, and the

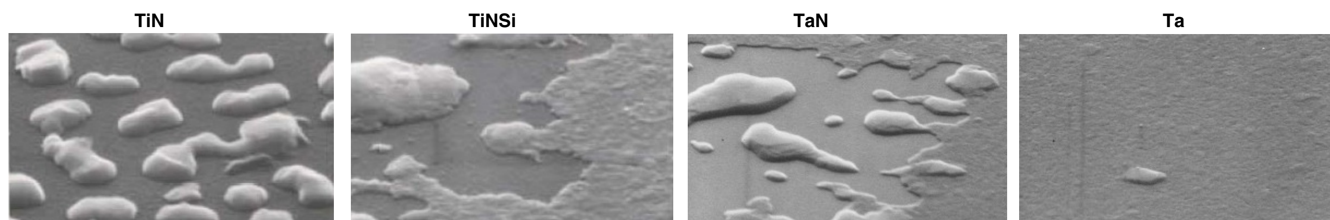

Figure 12. De-wetting experiments for 100 Å Cu on various barrier layers, annealed at 380 °C for 15 min show the best wetting for the Ta surface.

sum of energy of a single Cu atom and the energy of Ta surface in a supercell of the same size. We calculated this using both LDA and GGA potentials and allowed the surface atoms of Ta to relax while the Cu atom position was held constant [15, 16].

As shown in figure 13, the minimum of the adsorption energy for GGA was 20 kcal mol^{-1} higher and at a slightly larger distance from the surface than using the LDA approximation. The Cu atom did form a stable configuration at the distance of 1 Å from the beta-Ta surface, and thereby quantified the earlier analysis showing a higher affinity of Cu with the beta-Ta surface. In this final case, we identified the equilibrium structure for further study and optimization to improve the wetting properties.

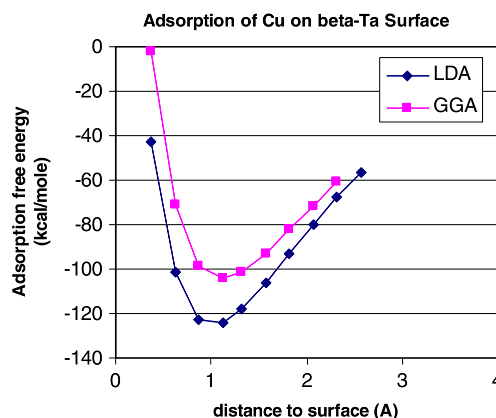

Figure 13. Adsorption energy of a Cu atoms on a beta-Ta(001) surface where the surface Ta atoms have been allowed to relax using both LDA and GGA pseudopotentials.

3. Summary and challenges in computational materials science

Although most of the problems in the nanoelectronics area involve properties extending beyond ground state atomic theory, several approximations are available for extension of DFT to excited states. DFT with generalized gradient approximation (GGA) and plane wave basis is the workhorse of applying condensed matter theory to realistic applications. As we demonstrated in two critical applications, DFT with suitable extensions may be used to investigate gas phase, surface, and gas–surface interactions. In addition, by appropriate multi-scale techniques, the analysis may be extended to realistic process systems at longer lengths and longer time steps. In our ALD application example, we used multi-scale modeling to simulate realistic deposition processes; (1) *ab initio* techniques estimated the electronic structure, (2) transition state theory estimated rates, (3) reaction–diffusion models modeled the deposition process. Depending on the rigor and accuracy of the components, the linked models are capable of length scales from ångströms to meters. In the demonstrated case, we effectively spanned about 10 orders of magnitude! The resulting models enabled extension of fundamental analysis for ALD reactor optimization. However, we did not address two other scales of models, in which the properties of the films and the electrical performance of the device may be predicted from *ab initio* methods. In a separate analysis, we evaluated interfacial adhesion strength of different films and predicted the film properties using DFT. We clearly demonstrated that nanotechnology development for semiconductor processing may be aided by judicious use of *ab initio* methods and integration of multiple scales. In the following section, we summarize some gaps and challenges to applying fundamental modeling for it to be completely predictive.

Materials modeling is needed to address four components; (1) synthesis to structure and composition, especially on interfaces, (2) properties of these structures including interface physics of state transition, defects states, etc, (3) transport properties from atomistic structure description, and finally (4) probing interactions with samples to enable quantification of structure and properties. As can be seen, the models span multiple scales and must be simulated using appropriate assumptions (figure 14). Most full quantum simulations may be done for smaller systems up to a few thousand atoms, which span approximately 30 nm^3. Currently, we use semi-empirical atomistic models to reach larger systems of millions of atoms. The potentials used in these models are characterized using both *ab initio* techniques and experiments. The applicability of atomistic models may be increased to over 100 million atoms by using more coarse-grained methods such as phase field based methods.

Materials modeling is applied at different levels of accuracy based on the requirements. High-performance materials applications require simultaneous optimization of multiple properties such as electronic, mechanical, and surface chemical reactivity among others. Some nanomaterials possess unique properties, making them optimal candidates to enhance or replace conventional materials and approaches, but the need for optimization of multiple properties requires models that correlate nanostructure to properties [3]. In early material

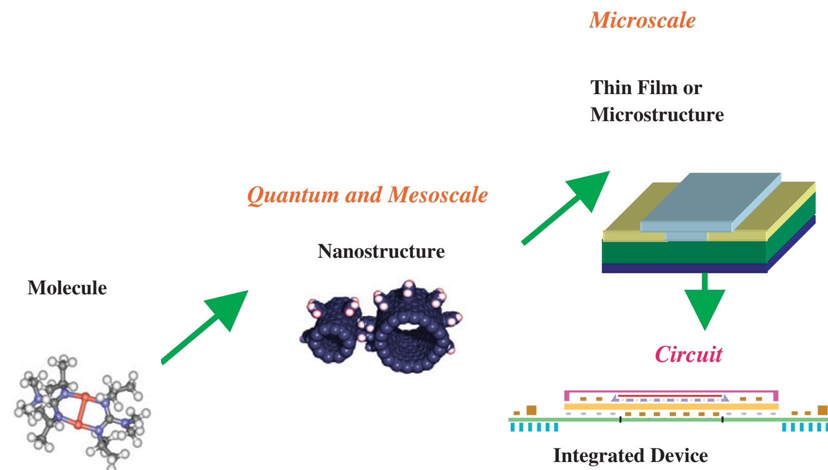

Figure 14. Multiple scales and the nature of models needed.

development, the need is to relate structure and chemistry to material properties. This is done in conjunction with specific metrology methods used to characterize the structures. In addition, the models are needed to optimize transient dynamics including film growth and transport of electrons, phonons, and atoms. In the second stage, the models are applied to improve the material to optimize structure, composition, and purity. Here as we mentioned above, the models relate structure, composition, and purity to properties. In the third stage, models are used to relate material properties to the functional properties of the device. Finally, the models at this stage, in conjunction with experimental observations, are used to optimize synthesis and integration.

Although material modeling is a critical part of technology development, the current state of the art limits its applications. As we illustrated, nanodevices themselves are constituted of nanostructures and involve integration of multiple materials and thin films. This is compounded by the fact that the film texture and crystallography are not well characterized. Generally, simulations are done using a modeler's intuition, experimental data, and statistical analysis. This is because most of the *ab initio* techniques are limited in their applications to estimate excited states, band gaps, and offsets for realistic material systems. In addition, bridging the various timescales to simulate fully dynamical or non-equilibrium systems such as electron transport or film growth are still outside the scope of some of the more advanced current techniques such as the *ab initio* molecular dynamics methods. The same problem is present in extending to the length scales as indicated above. This limits application of these models to interface properties of heterostructures and multiple stacked thin films. In addition, the ability to predict defects to the order of parts per million is beyond the current applicability of full quantum methods. The requirements for problem set-up, management, and analysis are also large. This is compounded by the fact that the different simulator tools in the materials modeling community do not link with each other in an open platform. We believe many opportunities exist in the area for a new paradigm beyond DFT that will scale linearly and also has predictive power for a wider class of materials. In addition, the community will benefit by coming together in an open platform in which different models, codes, and applications may exchange models and information with each other. These may enable tremendous success for computational material science to advance beyond the existing applications, increasing our ability to simulate fully integrated structures and longer timescale processes.

Acknowledgments

The authors would like to thank Dipto Thakurta for support with reactor simulations and Carolyn Duran for wetting experiments. In addition, we would like thank Jorge Garcia for management support of this activity.

References

[1] Feynman R P 1959 *There's Plenty of Room at the Bottom* American Physical Society, California Institute of Technology (Caltech)
[2] Simka H, Shankar S, Duran C and Haverty M 2005 Fundamentals of Cu/barrier-layer adhesion in microelectronic processing *Materials, Technology and Reliability of Advanced Interconnects* ed P R Besser, A J McKerrow, F Iacopi, C P Wong and J Vlassak (Vlassak, Mater. Res. Soc. Symp. Proc. vol 863, Warrendale, PA, USA)
[3] 2006 *Implementation Plan for Chemical Industry R&D Roadmap for Nanomaterials by Design*
[4] 2007 *International technology Roadmap for Semiconductors* sections on Emerging Research on Devices
[5] *International technology Roadmap for Semiconductors* sections on Emerging Research on Materials (2007)
[6] Hohenberg P and Kohn W 1964 *Phys. Rev.* **136** B864
[7] Kohn W and Sham L J 1965 *Phys. Rev.* **140** A1133
[8] Widjaja Y and Musgrave C B 2002 *Appl. Phys. Lett.* **80** 3304
[9] Elam J W, Groner M D and George S M 2002 *Rev. Sci. Instrum.* **73** 2981
[10] Copel M, Gribelyuk M and Gusev E 2000 *Appl. Phys. Lett.* **76** 436–8
[11] Ritala M, Leskela M, Dekker J, Mutsaers C, Soininen P J and Skarp J 1999 *Chem. Vapor Depos.* **5** 7
[12] Becke A D 1993 *J. Chem. Phys.* **98** 5648

[13] Frisch M J, Trucks G W, Schlegel H B, Scuseria G E, Robb M A, Cheeseman J R, Zakrzewski V G, Montgomery J A Jr, Stratmann R E, Burant J C, Dapprich S, Millam J M, Daniels A D, Kudin K N, Strain M C, Farkas O, Tomasi J, Barone V, Cossi M, Cammi R, Mennucci B, Pomelli C, Adamo C, Clifford S, Ochterski J, Petersson G A, Ayala P Y, Cui Q, Morokuma K, Salvador P, Dannenberg J J, Malick D K, Rabuck A D, Raghavachari K, Foresman J B, Cioslowski J, Ortiz J V, Baboul A G, Stefanov B B, Liu G, Liashenko A, Piskorz P, Komaromi I, Gomperts R, Martin R L, Fox D J, Keith T, Al-Laham M A, Peng C Y, Nanayakkara A, Challacombe M, Gill P M W, Johnson B, Chen W, Wong M W, Andres J L, Gonzalez C, Head-Gordon M, Replogle E S and Pople J A 2001 *Gaussian 98* (Pittsburgh, PA: Gaussian)

[14] Intel Website on 65 nm Technology http://www.intel.com/technology/architecture-silicon/65nm-technology/description.htm?iid=technology65nmmoveiview+tabs_description

[15] Kresse G and Furthmüller J 1996 *Comput. Mater. Sci.* **6** 15–50

[16] Kresse G and Furthmüller J 1996 *Phys. Rev.* B **54** 11169